





## Article

# Clinical and Histopathological Evolution of Acute Intraperitoneal Infection by *Streptococcus agalactiae* Serotypes Ib and III in Nile Tilapia

Natália Amoroso Ferrari <sup>1</sup>, Leonardo Mantovani Favero <sup>1</sup>, Cesar Toshio Facimoto <sup>1</sup>, Alais Maria Dall Agnol <sup>1</sup>, Marcos Letaif Gaeta <sup>1</sup>, Thalita Evani Silva de Oliveira <sup>2</sup>, Daniela Dib Gonçalves <sup>3</sup>, Nelson Maurício Lopera-Barrero <sup>4</sup>, Ulisses de Pádua Pereira <sup>1,\*</sup> and Giovana Wingeter Di Santis <sup>2,†</sup>

<sup>1</sup> Laboratory of Fish Bacteriology, Department of Preventive Veterinary Medicine, State University of Londrina, Londrina 86057-970, PR, Brazil; natalia.amoroso@uel.br (N.A.F.); leonardo\_mfavero@hotmail.com (L.M.F.); cesar.facimoto@hotmail.com (C.T.F.); alaisagnol@uel.br (A.M.D.A.); mlgaeta@uel.br (M.L.G.)

<sup>2</sup> Laboratory of Animal Pathology, Department of Preventive Veterinary Medicine, State University of Londrina, Londrina 86057-970, PR, Brazil; thalitamvet@gmail.com (T.E.S.d.O.); giovanaws@uel.br (G.W.D.S.)

<sup>3</sup> Department of Preventive Veterinary Medicine and Public Health, Paranaense University, Umuarama 87502-210, PR, Brazil; danieladib@unipar.br

<sup>4</sup> Department of Animal Science, State University of Londrina, Londrina 86057-970, PR, Brazil; nmlopera@uel.br

\* Correspondence: upaduapereira@uel.br; Tel.: +55-43-3371-4259

† These authors contributed equally to this work.

**Abstract:** *Streptococcus agalactiae* is a highly invasive bacterium that causes significant economic losses in tilapia aquaculture around the world. Furthermore, it is a pathogen for mammals, including humans, emphasizing its importance in One Health. The aim of this work was to evaluate the evolution of clinical and histopathological lesions caused by acute infection with two serotypes of *S. agalactiae*. For this, two strains isolated from natural outbreaks in Brazilian aquaculture farms (S13, serotype Ib; S73, serotype III) were used to challenge juvenile Nile tilapia (*Oreochromis niloticus*) intraperitoneally. Target organ samples were collected ten times, between 1 and 96 h post-infection, for microbiological and histopathological analyses. Anorexia was the first clinical sign and the first death occurred at 24 and 30 h in the fish infected with strains S13 and S73, respectively. Serotype Ib initially caused more pronounced lesions in the nervous system; however, serotype III lesions progressed more aggressively, reaching the same severity as those of serotype Ib. This trend was repeated in the mortality curve after 32 h. These results elucidated the important stages in the pathogenesis of *S. agalactiae* serotypes Ib and III in tilapia and suggest “tips and tricks” to improve the positive culture rate in the clinical diagnosis of infections in some tissues.

**Keywords:** streptococcosis; group B *Streptococcus*; pathogenesis; fish

**Key Contribution:** The experimental challenge with group B *Streptococcus agalactiae* in Nile tilapia (*Oreochromis niloticus*) caused an acute infection, mainly in the meninges and eyes, confirming the clinical signs of exophthalmos, erratic swimming, and systemic signs. When comparing serotypes Ib and III of *Streptococcus agalactiae*, the lesions caused by the serotype III strain were more severe compared to those of serotype Ib.



**Citation:** Ferrari, N.A.; Favero, L.M.; Facimoto, C.T.; Dall Agnol, A.M.; Gaeta, M.L.; de Oliveira, T.E.S.; Gonçalves, D.D.; Lopera-Barrero, N.M.; Pereira, U.d.P.; Di Santis, G.W. Clinical and Histopathological Evolution of Acute Intraperitoneal Infection by *Streptococcus agalactiae* Serotypes Ib and III in Nile Tilapia. *Fishes* **2024**, *9*, 279. <https://doi.org/10.3390/fishes9070279>

Academic Editor: Jiong Chen

Received: 11 June 2024

Revised: 11 July 2024

Accepted: 11 July 2024

Published: 13 July 2024



**Copyright:** © 2024 by the authors. Licensee MDPI, Basel, Switzerland. This article is an open access article distributed under the terms and conditions of the Creative Commons Attribution (CC BY) license (<https://creativecommons.org/licenses/by/4.0/>).

## 1. Introduction

Group B *Streptococcus agalactiae* (GBS) is a Gram-positive pathogen with coccoid morphology that was first isolated in cow's milk and cattle with mastitis. It is capable of causing a wide range of diseases in various animals, such as mammals, reptiles, amphibians, and fish [1]. In the human population, the incidence of events caused by GBS is increasing,

and it is one of the most important causes of death in newborns, as well as being a notable cause of death and morbidity in immunosuppressed adult patients [2].

*S. agalactiae* is divided into ten different serotypes depending on the type of capsular polysaccharide it possesses [3]. Each serotype has its own characteristics related to the type of host it infects, and its dominance may depend on its geographical region. Also, different genetic profiles have been studied, for instance by Multilocus Sequencing, and some specific sequence types are related to epidemiological niches and/or hosts, in addition to virulence level [4,5]. For fish, and in aquaculture, streptococcosis is one of the most important bacterial diseases, mainly for serotypes Ia, Ib, and III, which have been isolated from different fish species and have been the cause of several mass outbreaks, consequently having a significant economic impact due to the large number of deaths [6]. Serotype III ST 283 can also be considered zoonotic, since it is associated with events linked to the consumption of raw fish in Asia [7,8]. Furthermore, the same serotype (III) has been shown to be capable of becoming a multidrug-resistant pathogen, threatening not only fish production but public health [9].

Among the fish affected by streptococcosis, the Nile tilapia (*Oreochromis niloticus*) stands out for its susceptibility to massive outbreaks of GBS, with high mortality rates recorded in the Americas, Africa, and Asia [10–12]. This condition is made all the more critical by the fact that tilapia is one of the most cultivated fish in the world and is the most cultivated fish in aquaculture farms in Brazil [13,14]. Tilapia with streptococcosis may show various clinical signs, such as behavioral changes like lethargy, erratic swimming in a whirlpool or sideways and on the surface of the water, unilateral or bilateral scoliosis, ocular opacity, periorbital and intraocular hemorrhage, exophthalmos, and finally mortality [15,16].

Organs that can be affected by the disease are the branchial vessels, heart, spleen, brain and cranial cavity, kidney, liver, eyes, and skin on the caudal and cranial extremities. The lesions frequently observed in the affected organs are epicarditis, splenitis, choroiditis, and granulomatous or lymphohistiocytic meningitis, with inflammatory cell infiltrates [17]. In addition to these changes, bacteria can also be isolated from these organs, confirming their association with the observed lesions. Despite the knowledge of the clinical signs, little is known about the progression of lesions during infection, especially when comparing different serotypes of this pathogen. Therefore, microscopic tools, such as histopathology, can highlight the changes in the host's affected tissues during the invasion of the pathogen, contributing to the elucidation of the pathogenesis of streptococcosis in tilapia.

Therefore, the aim of this study was to evaluate the evolution of clinical signs and histopathological lesions in Nile tilapia after acute experimental infection with *S. agalactiae* serotypes Ib and III in order to observe the progression of the infection in the host organism.

## 2. Materials and Methods

### 2.1. Fish

A total of 120 Nile tilapia (*O. niloticus*), weighing  $55.35 \pm 0.7$  g, were obtained from a commercial hatchery in Paraná State, Brazil, without clinical signs of infectious diseases or a history of streptococcosis. A random sample of 10 fish was euthanized and submitted to bacterial diagnosis on blood agar with 5% sheep blood, which was incubated at 28 °C for 48 h. After observing negative results, the fish were divided into two tanks with 150 L (55 fish in each) and quarantined for 30 days under ideal conditions (pH = 6.8–7.2; total ammonia < 1 ppm; chlorine = 0; temperature =  $27 \pm 2$  °C; 12 h day–night photoperiod; fed three times a day with 2.0 mm commercial feed containing 36% crude protein). One of the tanks was used for the challenge with strain S13 (GBS serotype Ib) and the other with strain S73 (GBS serotype III). Observation of clinical signs and assembly rate, and collections for the histopathological analysis were carried out on animals allocated to the same tank.

## 2.2. Experimental Infection Design

Each group was infected with two different strains of streptococci, the S13 group and the S73 group, which had been previously isolated and characterized [9,18]. These strains were isolated from outbreaks with natural high mortality on tilapia farms in the south and northeast of Brazil, respectively. While serotype Ib was already reported in Brazil, strain S73, belonging to serotype III, was described for the first time in the country by our team and was characterized as multidrug-resistant, highly virulent, and belonging to ST 283 (unpublished data).

After immersion anesthesia using 50 mg L<sup>-1</sup> of benzocaine, the fish were intraperitoneally injected with 100 µL of bacterial culture in brain–heart infusion (BHI) broth with the following bacterial doses:  $4.3 \times 10^8$  colony-forming units (CFUs) per fish for S13 and  $3.43 \times 10^7$  CFUs per fish for S73, based on previous LD50 (lethal doses of 50% of the animals) experiments conducted by our team for each strain. A high dose was used to promote an acute infection in all the animals to enable the evaluate of clinical and lesion progression. The clinical signs and mortality of the fish were observed for seven days after the experimental infection. The fish were evaluated every hour (for first 48 hpi) and at least 5 times on the following days. The evaluation of clinical signs was performed by inspecting the animals and any changes observed were described according to Marcusso et al. [19].

This experiment was approved by the Animal Ethics Committee of the State University of Londrina (approval number: 19472.2015.51).

## 2.3. Sample Collection

Four fish (two from each tank) were euthanized before infection to be used as the control (0 h). In the challenged groups, after the inoculation, four fish from each group were collected at 1 h, 3 h, 6 h, 9 h, 12 h, 24 h, 36 h, 48 h, 72 h, and 96 h. Samples of the eye, brain, and head kidney from all fish were immediately streaked on 5% sheep blood agar for bacterial culture. Fragments of the eye, brain, liver, and spleen were fixed in 10% buffered formalin for histopathological analysis.

## 2.4. Histopathological Analysis

For microscopic examination, formalin-fixed paraffin-embedded tissue samples underwent routine processing. The paraffin blocks were cut into 5 µm sections and stained with hematoxylin–eosin (HE).

Microscopic changes were recorded, and to enhance objectivity in the assessment, specific parameters were considered for each evaluated organ. A scoring scale was then developed, encompassing the following criteria. The eye was checked for inflammation (0 to 3 points, from absent to accentuated), the extent (0 to 3 points, from absent to involvement of more than three structures), and the presence of exudate within the eye (0 to 1 point for each, absent or present). Within the nervous system, evaluations included checking for inflammation (0 to 3 points, from absent to accentuated), the extent (0 to 3 points, 0 for absent, 1 for meningitis, 2 for meningitis + encephalitis or ventriculitis, and 3 for all three combined), and the presence of exudate in the meninx, parenchyma, or ventriculus (0 to 1 point for each, absent or present). In the spleen assessment, particular attention was given to periarteriolar macrophage sheaths—PAMSs (0 to 4 points, from inconspicuous PAMSs to marked presence of PAMSs, with multiple cell layers, often coalescing), along with the detection of pigmented macrophage centers/aggregates—PMCs (0 to 3 points, from absent to frequent and large PMCs), and bacteria-laden macrophages—BLM (0 to 3 points, from absent to abundant). The hepatic analysis included the evaluation of glycogen storage (1 to 3 points, from normal glycogen storage to marked reduction, and/or presence of lipid accumulation), and checking for inflammation (0 to 3 points, from absent to accentuated). Group score values are represented by the arithmetical media of the samples. Statistical analysis of the data was performed using the non-parametric Kruskal–Wallis test, followed by Dunn’s test to verify whether the groups differed from each other. All detailed criteria descriptions can be found in Supplementary Table S1.

### 3. Results

#### 3.1. Clinical Signs and Mortality

Anorexia was observed 12 h after the start of the experimental challenge in both groups, and lethargic behavior was observed 27 h after the start in the S73 group and 32 h after the start in the S13 group (Table 1). The first fish death occurred 24 h after the start in the S13 group and 30 h after the start in the S73 group. Briefly, although mortality started earlier for the serotype Ib group, the mortality rate in the serotype III group reached and surpassed that of the serotype Ib group within 33 h of observation. It is also worth noting that both groups reached 100% mortality at 96 h (serotype III) and at 7 days (serotype Ib). The accumulated mortality for each experimental group is presented in Supplementary Figure S1. However, as the experiment was conducted with only one tank for each strain, it is important to highlight that these data only include the animals that died, and therefore, the fish that were used in the collection of biological material were not considered in the cumulative mortality. Corneal opacity was observed 48 h after the start in the S73 group and 80 h after the start in the S13 group. Severe exophthalmos was observed 72 h after the start in both groups, and erratic swimming was observed 80 h after the start in the S73 group and 6 days after the start in the S13 group (Figure 1). Other severe signs were observed after 7 days of infection: hyperesthesia and scoliosis in the S13 group, and corneal ulcers and fistulae in the S73 group.

**Table 1.** Onset of clinical signs observed in groups of Nile tilapia experimentally intraperitoneally infected with Group B *Streptococcus agalactiae* serotypes Ib (S13 strain) and III (S73 strain).

Clinical Sign	S13 (GBS Ib) Group	S73 (GBS III) Group
Anorexia	12 h	12 h
First death	24 h	30 h
Lethargy	32 h	27 h
Corneal opacity	80 h	48 h
Exophthalmos	72 h	72 h
Erratic swimming	6 d	80 h



**Figure 1.** Severe exophthalmos observed in experimental infection of Nile tilapia with group B *Streptococcus agalactiae*.

#### 3.2. Macroscopic Changes and Bacterial Recovery

Macroscopic changes were observed in the fishes in the first sampling (1 h after infection), when both strains caused head kidney congestion. Brain congestion was observed 3 h after the start in the S73 group and 12 h after the start in the S13 group. Hepatic congestion was observed 24 h after the start in the S73 group and 48 h after the start in the S13 group. The bacterial recovery rate from the fish after infection was 100% for the brain and head kidney, but it was less consistent from the eye, with no S73 detected in the first few hours in this organ and fluctuating values for S13 (Table 2).

**Table 2.** Reisolation rate of two strains of Group B *Streptococcus agalactiae* serotypes Ib (S13 strain) and III (S73 strain) after experimental infection in Nile tilapia.

Hours Post-Infection	Strain Recovery (%)					
	Brain		Kidney		Eye	
	S13	S73	S13	S73	S13	S73
01 h	4/4 (100)	4/4 (100)	4/4 (100)	4/4 (100)	1/4 (25)	0/4 (0.0)
03 h	4/4 (100)	4/4 (100)	4/4 (100)	4/4 (100)	0/4 (0.0)	0/4 (0.0)
06 h	4/4 (100)	4/4 (100)	4/4 (100)	4/4 (100)	1/4 (25)	0/4 (0.0)
09 h	4/4 (100)	4/4 (100)	4/4 (100)	4/4 (100)	1/4 (25)	3/4 (75)
12 h	4/4 (100)	4/4 (100)	4/4 (100)	4/4 (100)	1/4 (25)	3/4 (75)
24 h	4/4 (100)	4/4 (100)	4/4 (100)	4/4 (100)	4/4 (100)	3/4 (75)
36 h	4/4 (100)	4/4 (100)	4/4 (100)	4/4 (100)	2/4 (50)	4/4 (100)
48 h	4/4 (100)	4/4 (100)	4/4 (100)	4/4 (100)	2/4 (50)	3/4 (75)
72 h	4/4 (100)	4/4 (100)	4/4 (100)	4/4 (100)	2/4 (50)	4/4 (100)
96 h	4/4 (100)	4/4 (100)	4/4 (100)	4/4 (100)	3/4 (75)	4/4 (100)

### 3.3. Histopathological Analysis—Eye

In the control group, the histomorphological architecture of the ocular structures was preserved (Figure 2A), and rare eosinophils and pigmented macrophages were present, scattered in the iris, choroidal gland, and retro and peribulbar adipose and connective tissues (RPACT). Animals infected with strain S13 exhibited an early discrete increase in iris vascularity. A mild to moderate number of eosinophils and pigmented macrophages were observed in the iris, choroidal gland, and RPACT between 1 and 9 h post-infection (hpi). At 12 hpi, a more significant iritis with a predominance of macrophages was present in three of the four fish analyzed (Figure 2B). At 24 hpi, eosinophils, mononuclear cells, and pigmented macrophages were observed in the iris and choroidal glands at a mild to moderate degree. Between 36 and 72 hpi, mononuclear cells and pigmented macrophages were observed in moderate to accentuated proportions in the choroidal gland, RPACT, and optical nerve, with necrosis and granulomatous inflammation (Figure 2C). Eosinophils were also present in the iris, mildly to markedly, at these time points. At 72 hpi, bacteria engulfed by macrophages were detectable in the RPACT, choroidal gland, and vitreous (Figure 2D). At 96 hpi, the exudate became obvious, occupying the most of the vitreous (Figure 2E). Moderate to marked numbers of inflammatory cells were observed in all structures of the eye (panophthalmitis), with granulomatous exudate mainly in the choroid gland, RPACT, and chambers of the eye, which contained numerous bacteria engulfed by macrophages, highlighting the severity of the lesions in the tissues. The granulomatous exudate was present in all animals in the final hours.

In the animals infected with strain S73, histopathological lesions were observed in the eye from 1 h post-infection, starting with a mild increase in iris vascularization and the presence of eosinophils ranging from rare to moderate in quantity. This condition persisted until 6 hpi, when the animals presented, in addition to eosinophils, mononuclear cells and pigmented macrophages in some parts of the eye, iris (Figure 2F), choroidal gland, and RPACT. This state remained at 12 hpi. At 24 hpi, one of the four fishes presented, in addition to the alterations already mentioned, bacterial colonies, macrophage-engulfing bacteria, and infiltration of macrophages in moderate to severe degrees in the choroidal gland. From 36 hpi to the end of the observation period, this pattern of inflammatory response remained but progressively increased in severity and extent, with bacteria-rich granulomatous exudate in the RPACT (Figure 2G), choroidal gland, optic nerve (48 hpi), and chambers (72 hpi), culminating with panophthalmitis (72 to 96 hpi). Furthermore, septic thrombi were observed in some animals from 72 to 96 hpi (Figure 2H).

In the score analysis, inflammation and the extent of the lesions intensified starting from 36 hpi in both strains, S13 and S73. Additionally, bacteria were microscopically observed in the eyes of fish challenged with strain S13 from 72 hpi onwards, while with strain S73, it occurred starting from 24 hpi (Figure 3 and Supplementary Tables S2 and S3).

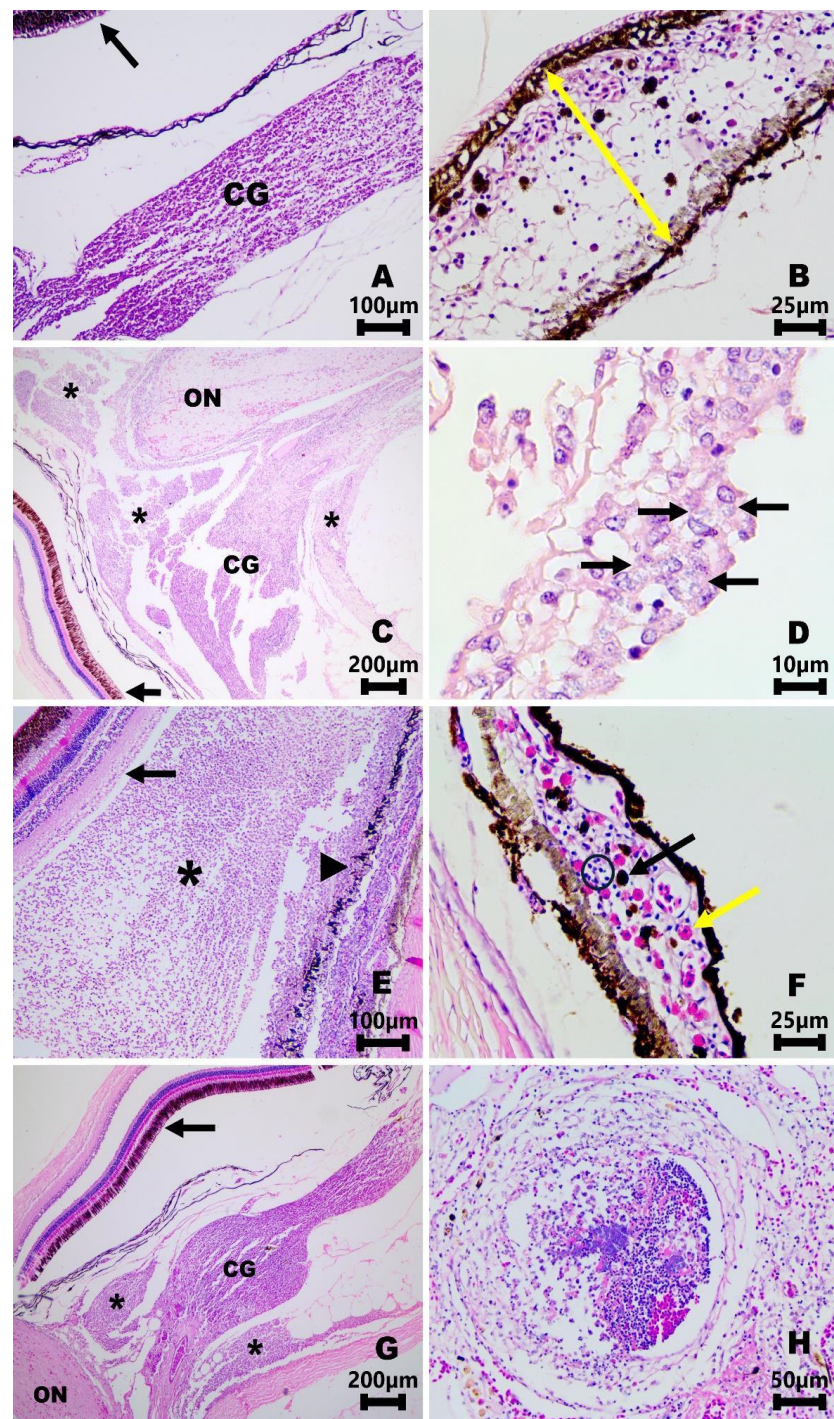


**Figure 2.** Histopathology of eye tissues from Nile tilapia (*Oreochromis niloticus*) that were uninfected (A) and experimentally infected with *Streptococcus agalactiae* serotype Ib S13 strain (B–E) and with *Streptococcus agalactiae* serotype III S73 strain (F–H) using hematoxylin–eosin (HE) staining. (A) Normal choroidal gland (CG), posterior segment of the retina (arrow), and retrobulbar adipose tissue with no evidence of inflammatory cells. There is an artifactual detachment of the structures, mainly the choroid and retina, with no injuries. Scale bar: 100  $\mu$ m; 10 $\times$ . (B) Iris at 12 h post-infection (hpi). Iris is thickened (yellow arrow) by edema, hyperemia, and inflammatory cell infiltration, mainly pigmented macrophages. Scale bar: 25  $\mu$ m; 40 $\times$ . (C) Eye fundus at 72 hpi. Marked accumulation of granulomatous exudate in the retrobulbar tissues (\*) between the choroidal gland (CG) and the retina (black arrow), and also affecting the optic nerve (ON). Scale bar: 200  $\mu$ m; 4 $\times$ . (D) Vitreous chamber at 72 hpi. Macrophages engulfing bacteria compound the exudate within the vitreous. Scale bar: 10  $\mu$ m;

100×. (E) Vitreous chamber at 96 hpi. Granulomatous exudate in the vitreous (\*) between the retina (black arrow) and iris (head arrow). Scale bar: 100 µm; 10×; (F) Iris at 6 hpi. Iris is thickened by edema, hyperemia, and inflammatory cell infiltration, mainly eosinophils (yellow arrow) with some pigmented macrophages (black arrow) and mononuclear cells (dotted circle). Scale bar: 25 µm; 40×. (G) Eye fundus at 48 hpi. Accumulation of moderate granulomatous exudate in the retrobulbar tissues (\*) between the choroidal gland (CG) and the retina (black arrow). The optic nerve (ON) was not affected in this animal. Scale bar: 200 µm; 4×. (H) Choroidal gland at 72 hpi. Septic thrombus in a damaged vessel; note bacterial colonies mixed with fibrin and leukocytes in the lumen. Scale bar: 50 µm; 20×.

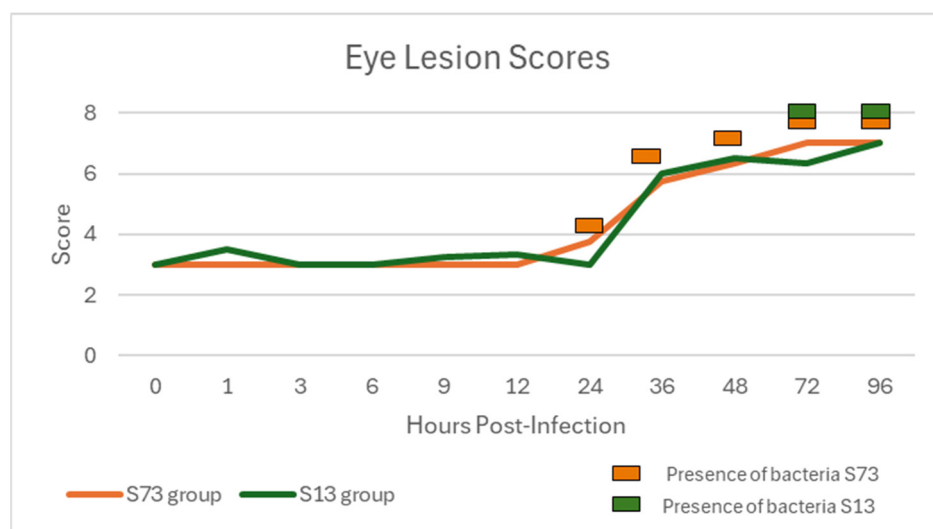


**Figure 3.** Analysis of the scores of histopathological lesions and presence of intralésional bacteria in the eye of Nile tilapia experimentally infected with Group B *Streptococcus agalactiae* serotypes Ib (S13 strain) and III (S73 strain).

### 3.4. Histopathological Analysis—Central Nervous System

In the control group, the meninges had a normal thickness, and no alterations were evident, except for rare detectable eosinophils in the meninges (Figure 4A). Between 1 and 24 h post-infection (hpi) with strain S13, vascular congestion and mild to moderate eosinophilic and mononuclear infiltrates were found in the meninges and parenchyma, mainly in the periventricular areas (Figure 4B) and in the brain stem. At 36 hpi, there was a conspicuous increase in meningeal inflammatory cell infiltration. Pigmented macrophages were also observed in the periencephalic tissues. Additionally, mild superficial infiltration of the brain parenchyma by inflammatory cells was present due to continuous meningeal inflammation. By 48 hpi, intense meningitis was evident, characterized by an increased meningeal thickness with a predominance of mononuclear infiltration, particularly macrophages. At 72 hpi, there was abundant granulomatous exudate extending from meninges to the periencephalic tissues (Figure 4C). Bacteria-engulfing macrophages were recognizable from this moment onward. At 96 hpi, at the peak of the inflammatory changes, the meningeal and periencephalic inflammatory infiltrates coalesced, covering the whole encephalon, and granulomatous exudate within the mesencephalic ventricle was common (Figure 4D,E). The encephalitis did not worsen compared to the previous time point. Also, regarding the statistical analysis, it was possible to observe significant differences when comparing the scores of the fish infected with the two serotypes only at 3 hpi ( $p$ -value: 0.02) and 6 hpi ( $p$ -value: 0.04), and only in the CNS.

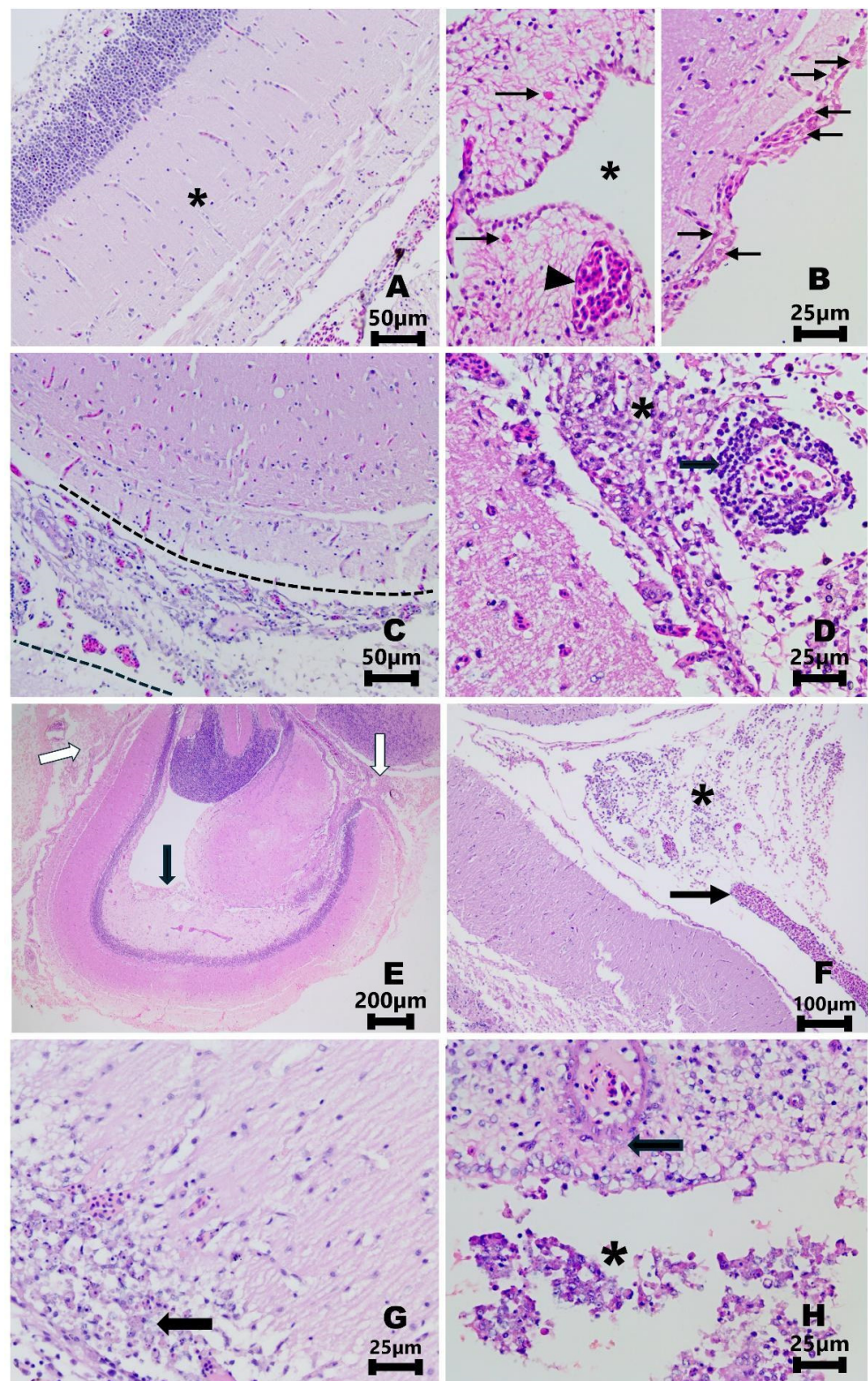


**Figure 4.** Histopathology of central nervous system (CNS) tissues from Nile tilapia (*Oreochromis niloticus*) that were uninfected (A) and experimentally infected with *Streptococcus agalactiae* serotype Ib S13 strain (B–E) and with *Streptococcus agalactiae* serotype III S73 strain (F–H) using hematoxylin–eosin (HE) staining. (A) Midbrain. Meninx is thin, with mild accentuation of vessels, and parenchyma is normal (\*). Scale bar: 50 µm; 20×. (B) Midbrain. Left: 24 h post-infection (hpi). Rare eosinophils (black arrows) and a hyperemic vessel (arrowhead) in the parenchyma adjacent to the third ventricle (\*). Right: 12 hpi. Some eosinophils (black arrows) are responsible for slight meningeal thickening.



Scale bar: 25  $\mu\text{m}$ ; 40 $\times$ . (C) Midbrain at 72 hpi. Marked meningeal thickening caused by inflammatory infiltrate predominantly comprised of macrophages and lymphocytes, edema, and congestion (between dashed lines). Scale bar: 50  $\mu\text{m}$ ; 20 $\times$ . (D) Cerebellar crest at 96 hpi. Thickening of the meninx is primarily caused by the infiltration of macrophages, with a higher concentration of lymphocytes in the perivascular areas. Scale bar: 25  $\mu\text{m}$ ; 40 $\times$ . (E) Midbrain at 96 hpi. There is severe meningitis with marked thickening due to inflammatory infiltrate (white arrows). Additionally, granulomatous inflammation is present within the ventricle (black arrow). Scale bar: 200  $\mu\text{m}$ ; 4 $\times$ . (F) Cerebellum at 48 hpi. Hyperemia (black arrow) and mononuclear inflammatory infiltrate (\*) resulting in meningeal thickening. Scale bar: 100  $\mu\text{m}$ ; 10 $\times$ . (G) Cerebellum at 96 hpi. Extension of the inflammatory process from the meninges into the parenchyma; inflammatory infiltrate, cells engulfing bacteria (black arrow), and molecular layer necrosis in the submeningeal region. Scale bar: 25  $\mu\text{m}$ ; 40 $\times$ . (H) Midbrain at 96 hpi. There is granulomatous inflammation in the ventricle with bacteria-engulfing macrophages and perivascular edema in the parenchyma due to a damaged vascular wall (black arrow). Scale bar: 25  $\mu\text{m}$ ; 40 $\times$ .

Fishes infected with serotype III (strain S73) developed mild to moderate congestion and only mild inflammatory changes, characterized mainly by scattered eosinophils in the meninges, from the first to the ninth hour after the challenge. At 12 hpi, mononuclear cells were incorporated into the inflammatory infiltrate, and segmental meningeal thickening was observed. By 24 hpi, the beginning of meningitis extension into the superficial brain parenchyma was noted. A more intense inflammation set in from 36 hpi onwards, with diffuse thickening of the meninges, extension of the inflammation into the periencephalic tissues, and the presence of colonies of bacteria and bacteria phagocytosed by macrophages, becoming more pronounced at 48 hpi (Figure 4F). This pattern was maintained until 72 hpi when perivascular cuffs and intercellular edema were observed. At 96 hpi, severe granulomatous meningitis and macrophages with a high number of intracytoplasmic bacteria were observed. The extension of this lesion to the superficial brain parenchyma made the encephalitis more obvious (Figure 4G). Additionally, intraventricular granulomatous exudate was prominent at this time point, with numerous bacteria-engulfing macrophages present in the exudate (Figure 4H).

In the scored analysis, the inflammation and extension of the lesions increased with time. The lesions started more discreetly in the group challenged with the S73 strain but increased during the experimental period. Bacteria in the CNS were only observed after 72 h in the S13 group, while in animals challenged with the S73 strain, it was observed from 36 h onwards (Figure 5 and Supplementary Tables S4 and S5).

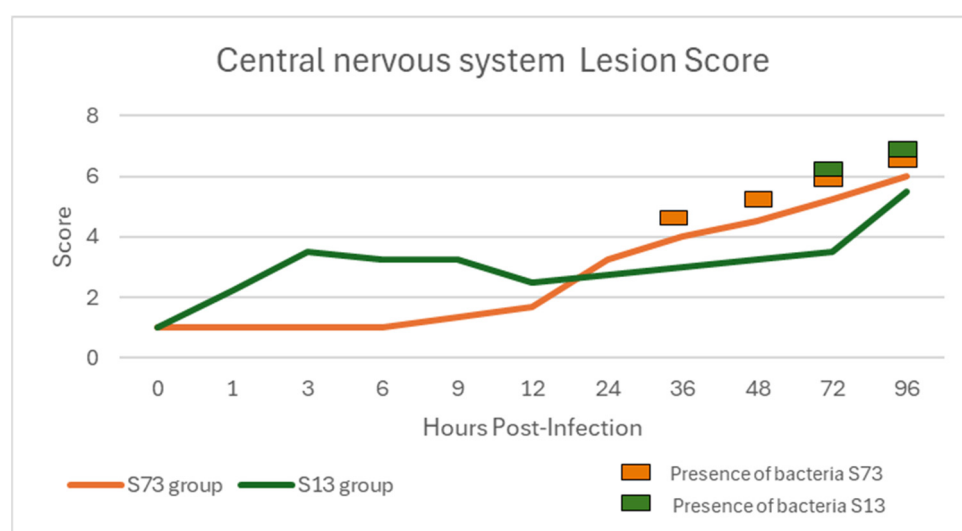


**Figure 5.** Analysis of the score of histopathological lesions and presence of intralésional bacteria in the central nervous system of Nile tilapia experimentally infected with Group B *Streptococcus agalactiae* serotypes Ib (S13 strain) and III (S73 strain).

### 3.5. Histopathological Analysis—Spleen

In the control group animals, the spleen exhibited white and red pulp in appropriate proportions, with undetectable periarteriolar macrophage sheaths (PAMSs). Pigmented macrophage centers (PMCs) were infrequent to common and typically small to medium in size, while scattered pigmented macrophages were abundant (Figure 6A).

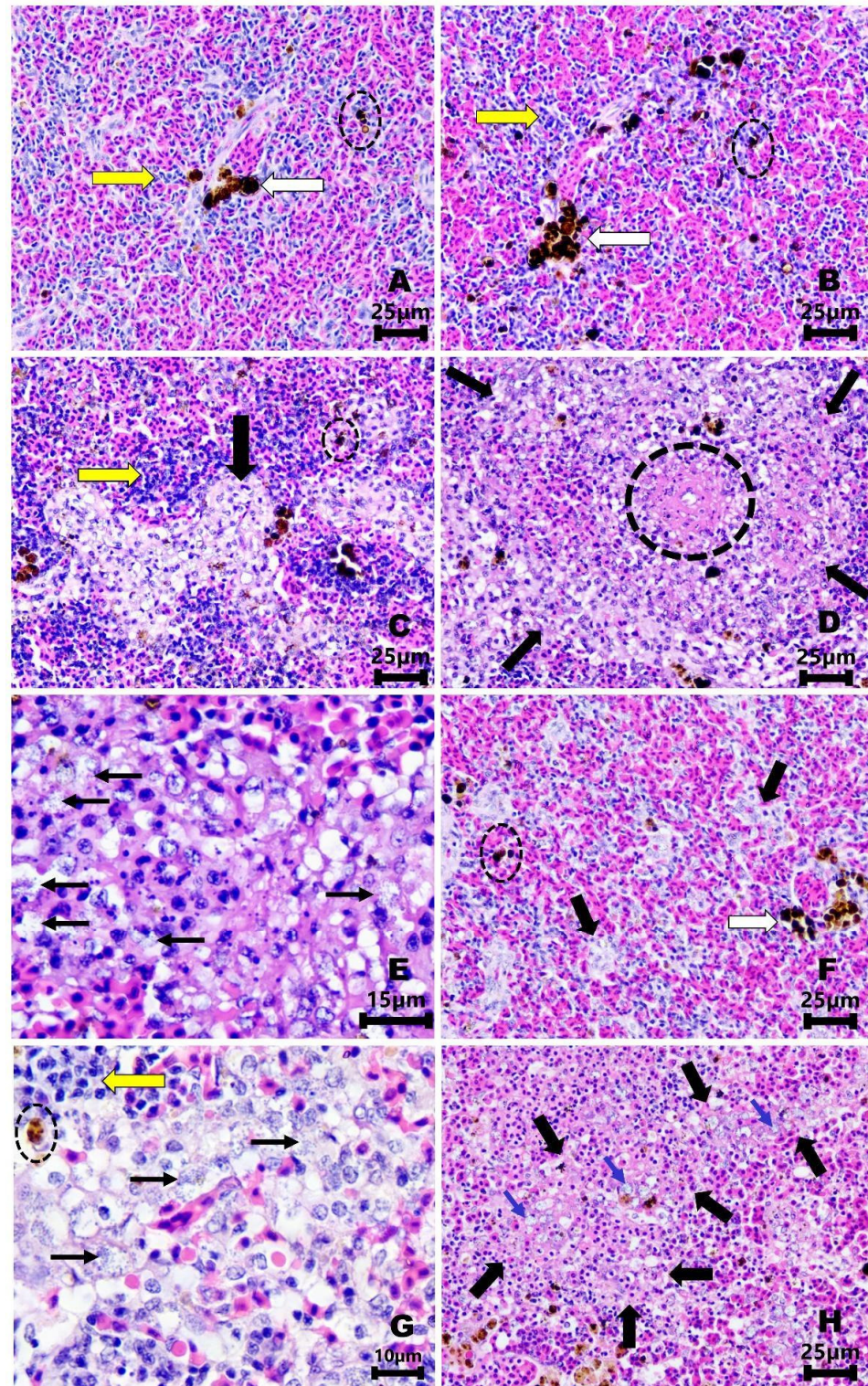


**Figure 6.** Histopathology of spleen tissues from Nile tilapia (*Oreochromis niloticus*) that were uninfected (A) and experimentally infected with *Streptococcus agalactiae* serotype Ib S13 strain (B–E) and with

*Streptococcus agalactiae* serotype III S73 strain (F–H) using hematoxylin–eosin (HE) staining. (A) Control group. Periarteriolar macrophage sheaths (PAMSs) are undetectable—score 0; pigmented macrophage centers (PMCs) are infrequent and small-sized—score 1 (white arrow); bacteria-laden macrophages are absent—score 0; and lymphocytes are abundant (yellow arrow). There are scattered pigmented macrophages (dashed circle). Scale bar: 25  $\mu$ m; 40 $\times$ . (B) One hour post-infection. The microscopic features are similar to those in the control sample. PAMSs are not distinguishable, PMC are medium-sized (white arrow), bacteria-laden macrophages are absent, and lymphocytes are abundant (yellow arrow). Scattered pigmented macrophages are common (dashed circle). Scale bar: 25  $\mu$ m; 40 $\times$ . (C) Six hours post-infection. Marked presence of PAMSs with many layers of cells, collapsing the vascular lumen—score 3. Lymphocytes are abundant and grouped around the PAMSs (yellow arrow). Bacteria-laden macrophages are present but are not easily discernible at this magnification. Scattered pigmented macrophages are common (dashed circle). Scale bar: 25  $\mu$ m; 40 $\times$ . (D) Twelve hours post-infection. Marked presence of coalescent, highly cellular PAMSs (score 4; black arrows), with fibrinoid necrosis (dashed circle). Scale bar: 25  $\mu$ m; 40 $\times$ . (E) Twenty-four hours post-infection. Abundant bacteria-laden macrophages (black arrows) and some cellular debris are present in the periarteriolar sheaths. Scale bar: 15  $\mu$ m; 100 $\times$ . (F) Three hours post-infection. PAMSs are evident, with two layers of cells and abundant cytoplasm—score 2 (black arrows). PMCs are small in size in this field (white arrow) and discrete pigmented macrophages are present (dashed circle). Red pulp is prominent, but lymphocytes are not so numerous. Scale bar: 25  $\mu$ m; 40 $\times$ . (G) Twelve hours post-infection. A PAMS region is rich in bacteria-laden macrophages (black arrows). Some groups of lymphocytes (yellow arrows) and scattered pigmented macrophages can also be observed. Scale bar: 10  $\mu$ m, 100 $\times$ . (H) Thirty-six hours post-infection. Markedly increased coalescent and highly cellular PAMSs (score 4; black arrows), effacing the typical architectural pattern of the organ. Bacteria-laden macrophages (blue arrows) and necrosis are common. Scale bar: 25  $\mu$ m; 40 $\times$ .

The spleen of animals infected with the strain S13 exhibited mild perisplenitis and congestion 1 h after intraperitoneal infection. From 1 to 3 hpi, PAMSs were subtle or not visible, but a small number of bacteria were already recognizable in some fish onward. PMCs were common to frequent and medium to large in size (Figure 6B), a pattern that persisted until the end of the experiment. At 6 hpi, the PAMSs became larger, more common, and more cellular. There was a decrease in the peripheral band of resident lymphocytes, which were now clustering around the PAMSs (Figure 6C). After 9 h of infection, the PAMSs progressively expanded towards the parenchyma, with a discrete number of bacteria present in the cytoplasm of the macrophages. At 12 hpi, necrotic foci, some fibrinoid, could be observed in the PAMSs. From this point until 48 hpi, the most severe grades were recorded for the PAMSs. Bacteria-laden macrophages became abundant, especially from 12 to 36 hpi, along with necrotic foci (Figure 6D,E). After 72 hpi, the tissue damage was reduced, with a decrease in the PAMSs, and a gradual reduction in the number of bacteria observed. PMCs continued to reach scores of 2 or 3, being common to frequent and medium to large in size.

In the group challenged with strain 73, splenic congestion was observed in the histopathological evaluation starting from 1 hpi. From 3 hpi on, there were some bacteria in the macrophages, and PAMSs became more conspicuous (Figure 6F), similar to the PMCs. At 9 hpi, perisplenitis containing a moderate number of eosinophils was also detected, progressing to granulomatous perisplenitis at 12 h after intraperitoneal infection. Between 12 and 36 hpi, the number of bacteria-laden macrophages progressively increased (Figure 6G), and the highest PAMS score persisted from 9 to 36 hpi (Figure 6H). At this point, the increase in size and the intensified coalescence of the PAMSs caused the loss of the spleen's normal architecture. A septic embolus was observed in one fish in each group from 36 to 96 hpi, with septic thrombus development in one of these fishes (72 hpi). There was a decrease in the severity of the lesions after 72 hpi; however, it was not as significant as in the group infected with the S13 strain.

In both experimental groups, the S13 and S73 groups, the highest scores were achieved between 9 and 48 hpi, with a decline after this period. The S13 strain group exhibited

bacterial presence in the splenic parenchyma at 1 hpi, whereas the S73 strain group showed it at 3 hpi, which persisted throughout the experiment in both group (Figure 7 and Supplementary Tables S8 and S9).

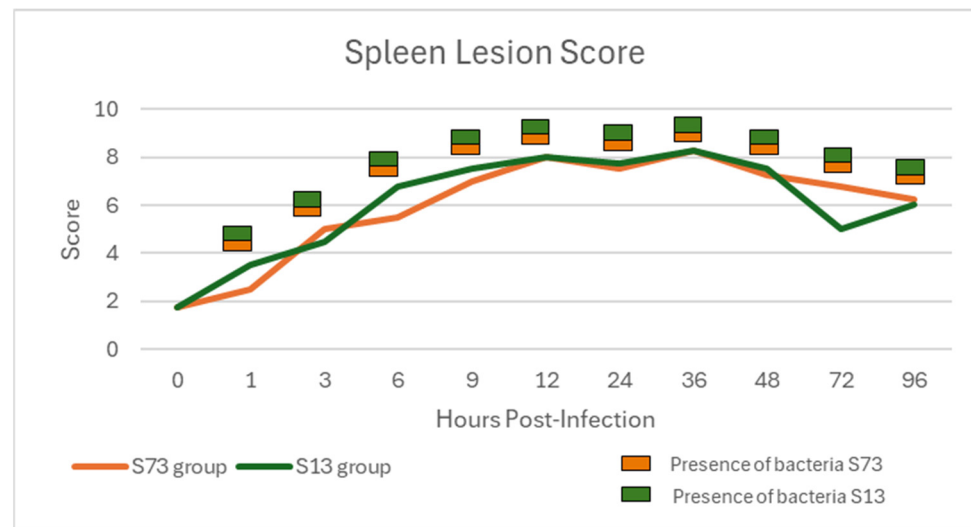


**Figure 7.** Analysis of the score of histopathological lesions in the spleen of Nile tilapia experimentally infected with Group B *Streptococcus agalactiae* serotypes Ib (S13 strain) and III (S73 strain).

### 3.6. Histopathological Analysis—Liver

In the control group, the hepatocytes exhibited an expanded and clear cytoplasm due to the pronounced storage of glycogen. With this pattern of accumulation, hepatocyte nuclei generally kept their central position, although they could be located paracentrally or peripherally, and they were compressed in the cellular rim (Figure 8A). Rare perivascular eosinophils and mononuclear cells were observed.

In the liver of the fish challenged with strain S13, abundant hepatocyte glycogen storage was observed between 0 and 6 hpi, at which point, focal perivascular inflammation was observed in one of the fish in the group (Figure 8B). From 9 to 24 hpi, the hepatocyte glycogen storage decreased in approximately 50% of the animals analyzed. In addition, the inflammation slightly increased, and hepatic vascular congestion was observed. Between 36 and 72 hpi, there was an infiltration of mononuclear cells, with the presence of macrophages engulfing bacteria and a predominance of perivascular macrophages in the hepatopancreas, highlighting the multifocal inflammation, endothelial injury, and vascular congestion (Figure 8C,D). Furthermore, at 96 h, lymphocytic inflammation was observed around vessels and the hepatopancreas, with marked hepatocyte glycogenic depletion and moderate to severe lipid accumulation in several animals (Figure 8E,F). Scattered hepatocyte necrosis and vascular congestion could be observed.

Similar to the lesions described in the group challenged with strain S13, there was also abundant hepatocyte glycogen storage in the tilapia challenged with strain S73, which became less evident throughout the infection. At 1 hpi, their liver tissue was similar to that of the control group (Figure 8G). As soon as 3 hpi, the first fish achieved an intermediate score for glycogen depletion, and by 24 hpi, the first fish had already reached the highest score (Figure 4H). At 24 hpi, hepatic congestion was accentuated, and macrophages containing bacteria and sinusoidal bacterial emboli were present (Figure 8H). At 72 h, there was discrete hepatocellular necrosis, and at 96 h, severe hepatocyte lipid accumulation was present in all the fish; nevertheless, inflammation did not become more severe.

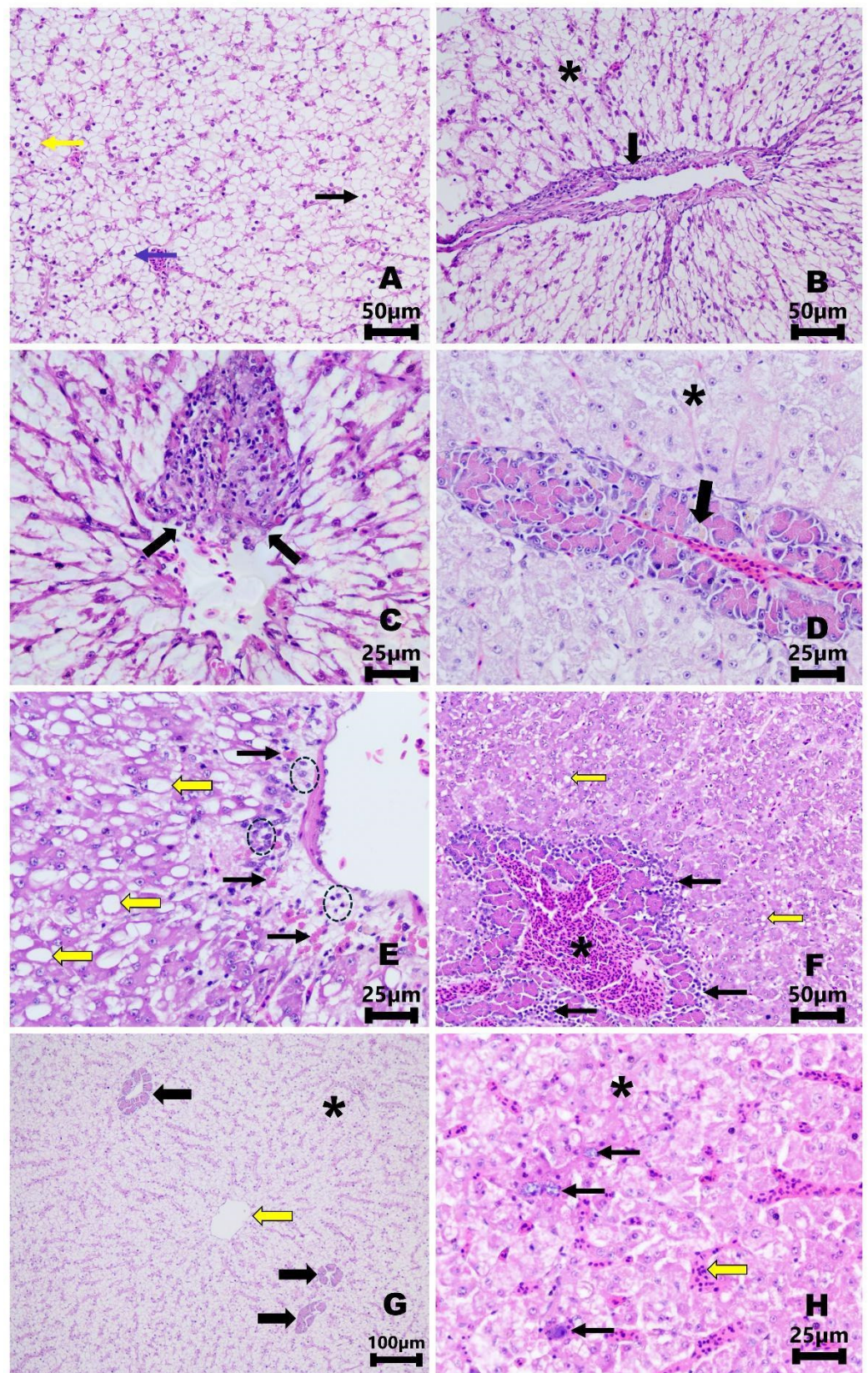


**Figure 8.** Histopathology of liver tissues from Nile tilapia (*Oreochromis niloticus*) that were uninfected (A) and experimentally infected with *Streptococcus agalactiae* serotype Ib S13 strain (B–F) and with *Streptococcus agalactiae* serotype III S73 strain (G,H) using hematoxylin–eosin (HE) staining. (A) Control group. Hepatocytes are extensively vacuolated due to accentuated glycogen storage—score 1.

The nuclei of these cells are located centrally (black arrow), paracentrally (yellow arrow), and even peripherally (blue arrow), but they are not narrowed. Scale bar: 50  $\mu\text{m}$ ; 20 $\times$ . (B) Six hours post-infection. Glycogen accumulation is marked—score 1 (\*). There is a thickening of the vascular wall due to the presence of inflammatory cells and edema (black arrow). Scale bar: 50  $\mu\text{m}$ ; 20 $\times$ . (C) Thirty-six hours post-infection. There is endothelial injury, vasculitis (black arrows), and perivascular extension of inflammatory cells. Scale bar: 25  $\mu\text{m}$ ; 40 $\times$ . (D) Thirty-six hours post-infection. Hepatocytes show slight cytoplasmic vacuolization due to decreased glycogen accumulation—score 2 (\*). Interspersed among the pancreatic acinar cells, some pigmented macrophages (black arrow) can be identified. Scale bar: 25  $\mu\text{m}$ ; 40 $\times$ . (E) Ninety-six hours post-infection. Hepatocytes display a significant decrease in glycogen storage and severe lipid accumulation—score 3. These cells exhibit large, distinct intracytoplasmic vacuoles, with nuclei that are either indistinct or compressed against the cytoplasmic periphery (yellow arrows). There are eosinophils (black arrows) and lymphocytes (dashed circles) in perivascular areas. Scale bar: 25  $\mu\text{m}$ ; 40 $\times$ . (F) Ninety-six hours post-infection. Hepatocytes exhibit widespread depletion of glycogen storage and lipid accumulation—score 3 (yellow arrow). At the periphery of a congested blood vessel (\*) unsheathed by pancreatic acini, there is pronounced inflammation characterized by a predominance of lymphocytes (black arrows). Scale bar: 50  $\mu\text{m}$ ; 20 $\times$ . (G) One hour post-infection. No lesions were observed in this sample. There is abundant glycogen storage (score 1) (\*), normal pancreatic acini (black arrows), and an unsheathed central vein. Scale bar: 100  $\mu\text{m}$ ; 10 $\times$ . (H) Twenty-four hours post-infection. Glycogen storage is significantly reduced (\*), accompanied by pronounced vascular congestion (yellow arrow), and the presence of some sinusoidal bacterial emboli (black arrows). Scale bar: 25  $\mu\text{m}$ ; 40 $\times$ .

In the scored analysis of the liver lesions, the scores increased throughout the experiment for the groups challenged with strain S13 and strain S73. The presence of bacteria in the liver parenchyma was only detected at 36 hpi in the fish challenged with strain S13, while in fish challenged with S73, it was noticed at 12 and 24 hpi. Among the four organs evaluated, the liver presented the mildest lesions (Figure 9 and Supplementary Tables S6 and S7).

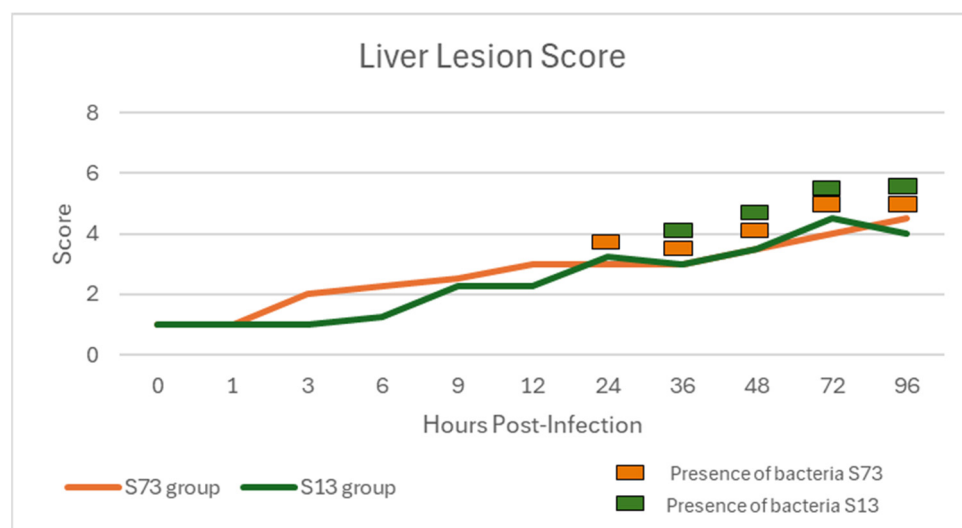


**Figure 9.** Analysis of the score of histopathological lesions and presence of intralésional bacteria in the liver of Nile tilapia experimentally infected with Group B *Streptococcus agalactiae* serotypes Ib (S13 strain) and III (S73 strain).

#### 4. Discussion

This study evaluated the evolution of the clinical signs and histopathological lesions in Nile tilapia after acute experimental infection with *S. agalactiae* serotypes Ib and III, from pre-challenge to 96 h post-infection. Streptococcosis is an aggressive disease for tilapia, causing severe mortality during outbreaks in farms, especially in the summer [9]. Clinical changes are evident in the eyes of affected fish and in systemic signs such as lethargy and erratic

swimming [17]. In this investigation, these changes were generally noticeable in the acute phase of the disease, starting around twelve hours after infection and persisting throughout the course of the streptococcosis. A study evaluated the histopathological lesions and erratic swimming in red tilapia (*Oreochromis* spp.) challenged with an intramuscular injection with  $10^8$  CFU/mL of GBS serotype III [20]. This dosage is similar to the one we used. The authors reported that all the fish presented erratic swimming between 6 h and 3 days post-infection, which is earlier than our results. Another group compared the clinical signs caused by *S. agalactiae* and *S. iniae* and concluded that the clinical symptoms caused by both species of *Streptococcus* spp. are very similar and cannot be used for the differential diagnosis of the disease [21]. In Indonesia, an experimental challenge with an injection of  $10^7$  CFU/mL of *S. agalactiae* and *S. iniae*, isolated from Nile tilapia cultured in net cages, demonstrated high pathogenicity in tilapia. Furthermore, all the challenged fish showed clinical signs and died within 6 days after infection. These results reinforce those obtained in this study and demonstrate the similarity in mortality rates in acute infections by *Streptococcus* spp. in another country [22].

Both bacteria strains were recovered at a rate of 100% from the central nervous system and head kidneys after only one hour of infection (Table 2). The recovery of both strains of GBS from the eyes varied, and at many time points, the bacteria were not recovered from any of the fish evaluated. These variations in the recovery rate of the bacteria from the eyes can be explained by the material used for isolation since bacterial isolation was carried out from an aliquot of the vitreous, and the histological changes found in this study and another experimental infection with *S. agalactiae* in tilapia showed that the bacteria infects the retro and peribulbar tissues in the early stages, and only reaches the ocular chambers later, manifesting as panophthalmitis [23]. These findings reinforce the need to collect tissues adjacent to the eye for more accurate and early bacteriological detection of *S. agalactiae* infection.

This severe inflammation of retro and peribulbar tissues has also been observed in more chronic cases affecting wild fish species such as the Giant Queensland grouper (*Epinephelus lanceolatus*), javelin grunter (*Pomadasydys kaakan*), and giant sea catfish (*Arius thalassinus*) [24], suggesting that the intense and characteristic exophthalmos of streptococcosis is a consequence of the panophthalmitis caused by the infection, and the severe involvement of the periorbital tissues, especially at the back of the eye.

Interestingly, it is possible to rule out the possibility of ocular infection via the optic nerve since the inflammatory findings present early in parts of the eye (e.g., iris, followed by the choroidal gland and RPACT), and tissue bacteria are detectable 24 h before any optic nerve lesions, which were observed at 72 hpi for the S13 strain and 36 hpi for the S73 strain. This reinforces the previously obtained results indicating that organ infection occurs hematogenously and not through direct entry via water [25].

Moreover, the observation of bacteria phagocytosed by macrophages in the eye tissues suggests that strain S73 (serotype III) can invade ocular tissues earlier than strain S13 (serotype Ib).

According to a previous study, *S. agalactiae* can survive in three ways in the host's blood: free, inside macrophages when phagocytosed, or attached to the inner wall of the vessels [23]. The internalization of bacteria by macrophages may allow them to be carried to the CNS, through a mechanism called the "Trojan horse," which facilitates the crossing of the blood-brain barrier (BBB) [26,27]. In this scenario, in addition to bacteria using macrophages to survive and evade the immune system, these cells also work to help spread the pathogen, taking it to other organs. For this reason, the mechanism was named "Trojan horse". Different bacterial strains of the same serotype may present varying degrees of virulence and infectivity among different tissues, including the CNS [26], and their interaction with macrophages may alter bacterial gene expression, for example, upregulating the expression of hyaluronate (HA) lyase, increasing the permeability of the BBB and favoring CNS invasion [28]. The ability of *S. agalactiae* to survive and multiply within macrophages maintains the bacteremia long enough to promote the development

of CNS infection [27,28]. This may explain the course of the lesions found in the CNS, which began with intense meningitis and, only hours later, extended due to the contiguity with the brain parenchyma, with some points of encephalitis. Although some studies relate streptococcal meningitis to the hematogenous route, few perivascular cuffs were observed in this study [26,29], suggesting that for the strains and conditions studied here, the gateway for BBB breakdown primarily occurred via the meninges.

Furthermore, severe granulomatous inflammation in the meninges, which was especially obvious in fish infected with the S73 strain, indicates that at four days, the disease was already in an advanced state, with alterations in brain functions. This, added to the periencephalic inflammation and the other lesions found in the brain, explains the neurological disturbances presented by the animals (erratic swimming and hyperesthesia) and reflects the intense mortality in this period [20,27]. Meningoencephalitis is associated with the high pathogenicity of GBS, due to the bacterium's ability to escape the immune barrier by endothelial destruction [30]. One study demonstrated that Brazilian GBS isolates have high infectivity and can escape the immune system [31]. Also, the S73 strain, isolated from an outbreak with a high mortality in Nile tilapia in Brazil, showed resistance to several classes of antimicrobials and zoonotic potential [9].

The spleen presented the earliest injuries in both challenged groups and as early as one hour after infection (S13 strain), bacteria were already found in the tissue. The spleen has an important function in the destruction of aged red blood cells and the capture of hematogenous pathogens [32].

Periarteriolar macrophage sheaths (PAMSs) and pigmented macrophage centers/aggregates (PMCs), also called melanomacrophage centers, are components of the splenic white pulp [33]. The exact function of each of these components is not well established; however, it is known that upon entering the spleen, pathogens first encounter the sheathed ellipsoids and subsequently the sinuses of the red pulp [34,35]. In this study, there was a noticeable increase in the PAMSs, with the presence of BLM progressively becoming more frequent between 9 and 48 h post-infection. Concurrently, there was an increase in PMCs, which persisted throughout the disease, although the observation of bacteria inside these cells was not common, perhaps obscured by intracytoplasmic pigment. Another study reported the extensive formation of melanomacrophage aggregates in the spleen of *Oreochromis mossambicus*, suggesting an intense stimulation of the immune response of this organ [28]. It is worth noting that *S. agalactiae* can survive and multiply within macrophages after being engulfed; these macrophages act as "Trojan horses" in spreading the pathogen [23].

Both *S. agalactiae* [26,36] and *S. iniae* [37] characteristically reside within phagocytes, especially macrophages, in large quantities, as observed in the spleen in this study. These infected cells either rupture or undergo apoptosis, likely through virulence mechanisms of the bacteria themselves, leading to the release of bacteria within the organ, facilitating their spread in the blood (bacteremia) to other organs. Another consequence is the reduced effectiveness of the immune response, as apoptotic macrophages will not perform their functions, and the presence of apoptotic bodies does not activate an inflammatory response as would occur with simple macrophage rupturing (which would result in the easy recognition of bacterial cells by new phagocytes) [28,36,37]. In this study, it was evident that at the moment when the spleen already presented severe lesions, including necrosis and vasculitis (around 12 hpi), in other organs, the lesions had not yet become severe, especially in the CNS, where they were more delayed, favoring the hypothesis that these previously mentioned mechanisms were present with the strains studied here. Thus, we suggest that the spleen be always included in this type of study due to its importance in understanding the pathogenesis of GBS infection.

The liver changes were mild, especially the inflammatory effects, as no fish evaluated in both experimental groups received the maximum score for inflammation. Even considering the animals that achieved the highest scores, in the final phases of the experiment, in both groups, these seem to reflect more of a systemic disease state, rather than an inflam-



matory lesion triggered directly by the pathogens, since the highest score came from the intracellular accumulations and not the inflammatory infiltrate. During the course of the disease, the animals lost their appetite and anorexia developed, leading to the consumption of the hepatic glycogen reserve and the mobilization of peripheral and visceral adipose tissue, with the consequent accumulation of lipids in hepatocytes (steatosis) [38]. This process has been observed previously in similar experiments, even with different pathogens [39]. Due to its nature and function, the liver is more exposed to pathogens and toxins coming from the digestive tract through the portal system [40]. A type of inflammation called nonspecific reactional hepatitis that can be found microscopically in dogs, for example, is characterized by the presence of a non-marked inflammatory infiltrate, as a response to the passage of pathogens through the liver, without there being specific hepatocellular or biliary tract damage [41]. There are no data in the literature that indicate that liver tissue, intrahepatic pancreatic tissue, or the biliary tract are specific targets for *S. agalactiae*; however, tissue damage could result from bacteremia, as explained previously. In this study, it was possible to recognize bacteria inside macrophages or sinusoidal emboli in only seven fish. Thus, despite the septicemic nature of the disease, severe liver damage does not appear to be common in acute infection with the strains studied; however, intrasinusoidal bacteria emboli were observed [26,36] and more significant lesions, including necrosis, can be noticed in more long-term experiments [42].

Comparing the two strains studied here, serotype III bacteria were identified earlier in the tissues of the eyes, brain, and liver than those of serotype Ib. Examining the histopathological lesions in the nervous system and eyes through a linear regression analysis, serotype Ib initially produced more pronounced lesions; however, serotype III lesions progressed more aggressively, eventually reaching the same severity as those of serotype Ib at 40 h post-infection. This trend is also reflected in the mortality curve (Figure 1), where serotype III surpasses serotype Ib in mortality by the 32 h mark. It is noteworthy that, after this period, several colonies were observed in the eyes of animals infected with serotype III (Figure 3). The ability of serotype III bacteria to break through the blood–brain barrier and blood–tissue barriers is probably greater. The genome from GBS serotype III that infects fish, such as S73 strain (NCBI accession number: CP030845), is approximately 14% larger than that of the GBS serotype Ib strain that was also isolated from fish (S13 strain; NCBI accession number: CP018623). Therefore, we speculate that this difference provides S73 a greater abundance of virulence factors related to strategies for escaping the host's immunological barriers [43], and therefore, standing out compared to strain S13.

## 5. Conclusions

Intraperitoneal experimental infection of tilapia with both serotypes of *Streptococcus agalactiae* resulted in acute infection, causing severe lesions, mainly in the meninges, eyes, and spleen, justifying the lethality of the infection. Despite this, it was possible to observe that, although serotype Ib caused earlier mortality, serotype III reached and exceeded the mortality rate by 32 hpi. In addition, GBS serotype III demonstrated greater systemic and tissue precocity bacteremia compared to serotype Ib, which was only able to cause more pronounced tissue lesions when the animals were already debilitated. In addition, this study made important contributions to facilitate more accurate microbiological diagnoses, as the results suggest that the meninges and periocular tissues are important collection points for reisolation of the pathogen in infections caused by GBS. These findings contribute to the knowledge on the pathogenesis and clinical evolution of streptococcosis caused by GBS serotypes Ib and III in Nile tilapia. However, it is necessary to characterize the genetic bases involved in the observed differences in the pathogenicity of the two serotypes using host–pathogen interaction approaches.

**Supplementary Materials:** The following supporting information can be downloaded at: <https://www.mdpi.com/article/10.3390/fishes9070279/s1>, Table S1: Scoring system for histopathological analysis of Nile tilapia experimentally infected with *Streptococcus agalactiae* serotypes Ib and III; Table S2: Score analysis of the histopathological lesions in the eye of Nile tilapia experimentally

infected with *Streptococcus agalactiae* serotype Ib—S13 strain. Values are the arithmetical media of the samples; Table S3: Score analysis of the histopathological lesions in the eye of Nile tilapia experimentally infected with *Streptococcus agalactiae* serotype III—S73 strain. Values are the arithmetical media of the samples; Table S4: Score analysis of the histopathological lesions in the central nervous system of Nile tilapia experimentally infected with *Streptococcus agalactiae* serotype Ib—S13 strain. Values are the arithmetical media of the samples; Table S5: Score analysis of the histopathological lesions in the central nervous system of Nile tilapia experimentally infected with *Streptococcus agalactiae* serotype III—S73 strain. Values are the arithmetical media of the samples; Table S6: Score analysis of the histopathological lesions in the liver of Nile tilapia experimentally infected with *Streptococcus agalactiae* serotype Ib—S13 strain. Values are the arithmetical media of the samples; Table S7: Score analysis of the histopathological lesions in the liver of Nile tilapia experimentally infected with *Streptococcus agalactiae* serotype III—S73 strain. Values are the arithmetical media of the samples; Table S8: Score analysis of the histopathological lesions in the spleen of Nile tilapia experimentally infected with *Streptococcus agalactiae* serotype Ib—S13 strain. Values are the arithmetical media of the samples; Table S9: Score analysis of the histopathological lesions in the spleen of Nile tilapia experimentally infected with *Streptococcus agalactiae* serotype III—S73 strain. Values are the arithmetical media of the samples. Figure S1: Mortality of Nile tilapia experimentally infected with Group B *Streptococcus agalactiae* serotypes Ib (S13 strain) and III (S73 strain).

**Author Contributions:** Conceptualization, U.d.P.P. and G.W.D.S.; methodology, L.M.F., C.T.F., M.L.G. and T.E.S.d.O.; formal analysis, L.M.F. and N.A.F.; investigation, L.M.F.; writing—original draft preparation, N.A.F., L.M.F. and A.M.D.A.; writing—review and editing, U.d.P.P. and G.W.D.S.; visualization, D.D.G. and N.M.L.-B.; supervision, U.d.P.P. and G.W.D.S.; project administration, U.d.P.P. and G.W.D.S. All authors have read and agreed to the published version of the manuscript.

**Funding:** This research was funded by the National Council for Scientific and Technological Development (CNPq), grant number 306857/2021-9.

**Institutional Review Board Statement:** The animal study protocol was approved by the Ethics Committee on Animal Use of the State University of Londrina (approval number: CEUA-UEL 2019472.2015.51).

**Data Availability Statement:** Data are contained within the article and Supplementary Materials.

**Acknowledgments:** The authors would like to acknowledge the Postgraduate Program in Animal Health and Production Science for its help and support in the research presented in this manuscript. The authors thank the National Council of Technological and Scientific Development (CNPq) for their financial support. Pereira, U.P. is a recipient of a CNPq Fellowship.

**Conflicts of Interest:** The authors declare no conflicts of interest.

## Abbreviations

BBB: blood–brain barrier; BHI: brain–heart infusion; BLM: bacteria-laden macrophages; CFU: colony-forming unit; CG: choroidal gland; CNS: central nervous system; GBS: group B *Streptococcus agalactiae*; HA: hyaluronate; HE: hematoxylin–eosin; hpi: hours post-infection; NCBI: National Center for Biotechnology Information; ON: optic nerve; PAMS: periarterial macrophage sheath; PMC: pigmented macrophage center/aggregate; RPACT: retro and peribulbar adipose and connective tissues.

## References

1. Lancefield, R.C. A serological differentiation of human and other groups of hemolytic streptococci. *J. Exp. Med.* **1933**, *57*, 571–595. [[CrossRef](#)] [[PubMed](#)]
2. Rao, G.G.; Khanna, P. To screen or not to screen women for Group B Streptococcus (*Streptococcus agalactiae*) to prevent early onset sepsis in newborns: Recent advances in the unresolved debate. *Ther. Adv. Infect. Dis.* **2020**, *7*, 2049936120942424. [[CrossRef](#)] [[PubMed](#)]
3. Slotved, H.-C.; Kong, F.; Lambertsen, L.; Sauer, S.; Gilbert, G.L. Serotype IX, a proposed new *Streptococcus agalactiae* serotype. *J. Clin. Microbiol.* **2007**, *45*, 2929–2936. [[CrossRef](#)] [[PubMed](#)]
4. Leal, C.A.; Queiroz, G.A.; Pereira, F.L.; Tavares, G.C.; Figueiredo, H.C. *Streptococcus agalactiae* sequence type 283 in farmed fish, Brazil. *Emerg. Infect. Dis.* **2019**, *25*, 776. [[CrossRef](#)] [[PubMed](#)]
5. Lusiastuti, A.M.; Textor, M.; Seeger, H.; Akineden, Ö.; Zschöck, M. The occurrence of *Streptococcus agalactiae* sequence type 261 from fish disease outbreaks of tilapia *Oreochromis niloticus* in Indonesia. *Aquac. Res.* **2014**, *45*, 1260–1263. [[CrossRef](#)]

6. Godoy, D.; Carvalho-Castro, G.; Leal, C.; Pereira, U.; Leite, R.; Figueiredo, H. Genetic diversity and new genotyping scheme for fish pathogenic *Streptococcus agalactiae*. *Lett. Appl. Microbiol.* **2013**, *57*, 476–483. [[CrossRef](#)] [[PubMed](#)]
7. Kalimuddin, S.; Chen, S.L.; Lim, C.T.K.; Koh, T.H.; Tan, T.Y.; Kam, M.; Wong, C.W.; Mehershahi, K.S.; Chau, M.L.; Ng, L.C.; et al. 2015 epidemic of severe *Streptococcus agalactiae* sequence type 283 infections in Singapore associated with the consumption of raw freshwater fish: A detailed analysis of clinical, epidemiological, and bacterial sequencing data. *Clin. Infect. Dis.* **2017**, *64*, S145–S152. [[CrossRef](#)] [[PubMed](#)]
8. Law, G.W.; Wijaya, L.; Tan, A.H.C. Group B Streptococcal prosthetic knee joint infection linked to the consumption of raw fish. *J. Orthop. Case Rep.* **2017**, *7*, 54–57.
9. Chideroli, R.T.; Amoroso, N.; Mainardi, R.M.; Suphoronski, S.A.; de Padua, S.B.; Alfieri, A.F.; Alfieri, A.A.; Mosela, M.; Morales, A.T.P.; de Oliveira, A.G.; et al. Emergence of a new multidrug-resistant and highly virulent serotype of *Streptococcus agalactiae* in fish farms from Brazil. *Aquaculture* **2017**, *479*, 45–51. [[CrossRef](#)]
10. Alazab, A.; Sadat, A.; Younis, G. Prevalence, antimicrobial susceptibility, and genotyping of *Streptococcus agalactiae* in Tilapia fish (*Oreochromis niloticus*) in Egypt. *J. Adv. Vet. Anim. Res.* **2022**, *9*, 95–103. [[CrossRef](#)]
11. Chen, M.; Wang, R.; Luo, F.G.; Huang, Y.; Liang, W.W.; Huang, T.; Lei, A.Y.; Gan, X.; Li, L.P. *Streptococcus agalactiae* isolates of serotypes Ia, III and V from human and cow are able to infect tilapia. *Vet. Microbiol.* **2015**, *180*, 129–135. [[CrossRef](#)] [[PubMed](#)]
12. Jaglarz, A.; Gurgul, A.; Leigh, W.J.; Costa, J.Z.; Thompson, K.D. Complete Genome Sequences of Three Fish-Associated *Streptococcus agalactiae* Isolates. *Genome Announc.* **2018**, *6*. [[CrossRef](#)] [[PubMed](#)]
13. ANUÁRIO 2024. Anuário Brasileiro da Piscicultura PEIXE BR 2024. Available online: <https://www.peixebr.com.br/anuario-2024/> (accessed on 25 June 2024).
14. Calixto, E.S.; Santos, D.F.B.; Lange, D.; Galdiano, M.S.; Rahman, I.U. Aquaculture in Brazil and worldwide: Overview and perspectives. *J. Environ. Anal. Progr.* **2020**, *5*, 98–107. [[CrossRef](#)]
15. Evans, J.J.; Klesius, P.H.; Gilbert, P.M.; Shoemaker, C.A.; Al Sarawi, M.A.; Landsberg, J.; Duremdez, R.; Al Marzouk, A.; Al Zenki, S. Characterization of  $\beta$ -haemolytic Group B *Streptococcus agalactiae* in cultured seabream, *Sparus auratus* L., and wild mullet, *Liza klunzingeri* (Day), in Kuwait. *J. Fish Dis.* **2002**, *25*, 505–513. [[CrossRef](#)]
16. Kayansamruaj, P.; Dinh-Hung, N.; Srisapoome, P.; Na-Nakorn, U.; Chatchaiphan, S. Genomics-driven prophylactic measures to increase streptococcosis resistance in tilapia. *J. Fish Dis.* **2023**, *46*, 597–610. [[CrossRef](#)] [[PubMed](#)]
17. Soto, E.; Zayas, M.; Tobar, J.; Illanes, O.; Yount, S.; Francis, S.; Dennis, M.M. Laboratory-controlled challenges of Nile Tilapia (*Oreochromis niloticus*) with *Streptococcus agalactiae*: Comparisons between immersion, oral, intracoelomic and intramuscular routes of infection. *J. Comp. Pathol.* **2016**, *155*, 339–345. [[CrossRef](#)] [[PubMed](#)]
18. Facimoto, C.T.; Chideroli, R.T.; Gonçalves, D.D.; Carmo, A.O.D.; Kalaphotakis, E.; Pereira, U.P. Whole-Genome Sequence of *Streptococcus agalactiae* Strain S13, Isolated from a Fish Eye from a Nile Tilapia Farm in Southern Brazil. *Genome Announc.* **2017**, *5*, 1–17. [[CrossRef](#)] [[PubMed](#)]
19. Marcusso, P.F.; Salvador, R.; de Almeida Marinho-Neto, F. Infecção por *Streptococcus agalactiae* em tilápias do Nilo (*Oreochromis niloticus*). *Rev. Ciênc. Agrovet.* **2017**, *16*, 165–169. [[CrossRef](#)]
20. Palang, I.; Withyachumnarnkul, B.; Senapin, S.; Sirimanapong, W.; Vanichviriyakit, R. Brain histopathology in red tilapia *Oreochromis* sp. experimentally infected with *Streptococcus agalactiae* serotype III. *Microsc. Res. Tech.* **2020**, *83*, 877–888. [[CrossRef](#)]
21. Chen, C.; Chao, C.; Bowser, P. Comparative histopathology of *Streptococcus iniae* and *Streptococcus agalactiae*-infected tilapia. *Bull. Eur. Assoc. Fish Pathol.* **2007**, *27*, 2.
22. Anshary, H.; Kurniawan, R.A.; Sriwulan, S.; Ramli, R.; Baxa, D.V. Isolation and molecular identification of the etiological agents of streptococcosis in Nile tilapia (*Oreochromis niloticus*) cultured in net cages in Lake Sentani, Papua, Indonesia. *Springerplus* **2014**, *3*, 1–11. [[CrossRef](#)] [[PubMed](#)]
23. Abdullah, S.; Omar, N.; Yusoff, S.M.; Obukwho, E.B.; Nwunuji, T.P.; Hanan, L.; Samad, J. Clinicopathological features and immunohistochemical detection of antigens in acute experimental *Streptococcus agalactiae* infection in red tilapia (*Oreochromis* spp.). *Springerplus* **2013**, *2*, 286. [[CrossRef](#)] [[PubMed](#)]
24. Bowater, R.O.; Forbes-Faulkner, J.; Anderson, I.G.; Condon, K.; Robinson, B.; Kong, F.; Gilbert, G.L.; Reynolds, A.; Hyland, S.; McPherson, G.; et al. Natural outbreak of *Streptococcus agalactiae* (GBS) infection in wild giant Queensland grouper, *Epinephelus lanceolatus* (Bloch), and other wild fish in Northern Queensland, Australia. *J. Fish Dis.* **2012**, *35*, 173–186. [[CrossRef](#)] [[PubMed](#)]
25. Iregui, C.A.; Vasquez, G.M.; Rey, A.L.; Verjan, N. Piscirickettsia-like organisms as a cause of acute necrotic lesions in Colombian tilapia larvae. *J. Vet. Diagn. Investig.* **2011**, *23*, 147–151. [[CrossRef](#)] [[PubMed](#)]
26. Cao, J.; Liu, Z.; Zhang, D.; Guo, F.; Gao, F.; Wang, M.; Yi, M.; Lu, M. Distribution and localization of *Streptococcus agalactiae* in different tissues of artificially infected tilapia (*Oreochromis niloticus*). *Aquaculture* **2022**, *546*, 737370. [[CrossRef](#)]
27. Eto, S.F.; Fernandes, D.C.; Moraes, A.C.; Alecrim, J.; Souza, P.G.; Carvalho, F.C.A.; Charlie-Silva, I.; Belo, M.A.A.; Pizauro, J.M. Meningitis Caused by *Streptococcus agalactiae* in Nile Tilapia (*Oreochromis niloticus*): Infection and inflammatory response. *Animals* **2020**, *10*, 2166. [[CrossRef](#)]
28. Guo, C.M.; Chen, R.R.; Kalhor, D.H.; Wang, Z.F.; Liu, G.J.; Lu, C.P.; Liu, Y.J. Identification of genes preferentially expressed by highly virulent piscine *Streptococcus agalactiae* upon interaction with macrophages. *PLoS ONE* **2014**, *9*, e87980. [[CrossRef](#)] [[PubMed](#)]

29. Laith, A.A.; Ambak, M.A.; Hassan, M.; Sheriff, S.M.; Nadirah, M.; Draman, A.S.; Wahab, W.; Ibrahim, W.N.; Aznan, A.S.; Jabar, A.; et al. Molecular identification and histopathological study of natural *Streptococcus agalactiae* infection in hybrid tilapia (*Oreochromis niloticus*). *Vet. World* **2017**, *10*, 101–111. [[PubMed](#)]
30. Wang, J.; Wu, J.; Yi, L.; Hou, Z.; Li, W. Pathological analysis, detection of antigens, FasL expression analysis and leucocytes survival analysis in tilapia (*Oreochromis niloticus*) after infection with green fluorescent protein labeled *Streptococcus agalactiae*. *Fish Shellfish Immunol.* **2017**, *62*, 86–95. [[CrossRef](#)]
31. Mian, G.F.; Godoy, D.T.; Leal, C.A.; Yuhara, T.Y.; Costa, G.M.; Figueiredo, H.C. Aspects of the natural history and virulence of *S. agalactiae* infection in Nile tilapia. *Vet. Microbiol.* **2009**, *136*, 180–183. [[CrossRef](#)]
32. Mebius, R.E.; Kraal, G. Structure and function of the spleen. *Nat. Rev. Immunol.* **2005**, *5*, 606–616. [[CrossRef](#)] [[PubMed](#)]
33. Bjørgen, H.; Koppang, E.O. Anatomy of teleost fish immune structures and organs. *Immunogenetics* **2021**, *73*, 53–63. [[CrossRef](#)] [[PubMed](#)]
34. Agius, C.; Roberts, R.J. Melano-macrophage centres and their role in fish pathology. *J. Fish Dis.* **2003**, *26*, 499–509. [[CrossRef](#)] [[PubMed](#)]
35. Lamers, C.H.; De Haas, M.J. Antigen localization in the lymphoid organs of carp (*Cyprinus carpio*). *Cell. Tissue Res.* **1985**, *242*, 491–498. [[CrossRef](#)] [[PubMed](#)]
36. He, Y.; Huang, J.-L.; Wang, K.-Y.; Chen, D.-F.; Geng, Y.; Huang, X.-L.; Ou-Yang, P.; Zhou, Y.; Wang, J.; Min, J. Pathogenicity of *Streptococcus agalactiae* in *Oreochromis niloticus*. *Oncotarget* **2017**, *5*, 401–413. [[CrossRef](#)]
37. Zlotkin, A.; Chilmonczyk, S.; Eyngor, M.; Hurvitz, A.; Ghittino, C.; Eldar, A. Trojan horse effect: Phagocyte-mediated *Streptococcus iniae* infection of fish. *Infect. Immun.* **2003**, *71*, 2318–2325. [[CrossRef](#)] [[PubMed](#)]
38. Dias, W.J.; Baviera, A.M.; Zanon, N.M.; Galban, V.D.; Garófalo, M.A.; Machado, C.R.; Bailão, E.F.; Kettelhut, I.C. Lipolytic response of adipose tissue and metabolic adaptations to long periods of fasting in red tilapia (*Oreochromis* sp., Teleostei: Cichlidae). *Anais da Academia Brasileira de Ciências* **2016**, *88*, 1743–1754. [[CrossRef](#)] [[PubMed](#)]
39. Favero, L.M.; Facimoto, C.T.; Chideroli, R.T.; da Costa, A.R.; Umezu, D.F.; Honda, B.T.B.; de Oliveira, A.G.; Flaiban, K.K.M.d.C.; Di Santis, G.W.; Pereira, U.d.P. Administration of dehydrated oxytetracycline effectively reduces francisellosis mortality in Nile tilapia. *Aquac. Res.* **2021**, *52*, 4116–4126. [[CrossRef](#)]
40. Sales, C.F.; Silva, R.F.; Amaral, M.G.C.; Domingos, F.F.T.; Ribeiro, R.I.M.A.; Thomé, R.G.; Santos, H.B. Comparative histology in the liver and spleen of three species of freshwater teleost. *Neotrop. Ichthyol.* **2017**, *15*, 1–12. [[CrossRef](#)]
41. Cullen, J.M. Summary of the World Small Animal Veterinary Association standardization committee guide to classification of liver disease in dogs and cats. *Vet. Clin. N. Am. Small Anim. Pract.* **2009**, *39*, 395–418. [[CrossRef](#)]
42. Su, Y.; Feng, J.; Liu, C.; Li, W.; Xie, Y.; Li, A. Dynamic bacterial colonization and microscopic lesions in multiple organs of tilapia infected with low and high pathogenic *Streptococcus agalactiae* strains. *Aquaculture* **2017**, *471*, 190–203. [[CrossRef](#)]
43. Korir, M.L.; Knupp, D.; LeMerise, K.; Boldenow, E.; Loch-Carusio, R.; Aronoff, D.M.; Manning, S.D. Association and virulence gene expression vary among serotype III group B streptococcus isolates following exposure to decidual and lung epithelial cells. *Infect. Immun.* **2014**, *82*, 4587–4595. [[CrossRef](#)] [[PubMed](#)]

**Disclaimer/Publisher’s Note:** The statements, opinions and data contained in all publications are solely those of the individual author(s) and contributor(s) and not of MDPI and/or the editor(s). MDPI and/or the editor(s) disclaim responsibility for any injury to people or property resulting from any ideas, methods, instructions or products referred to in the content.